Available online at www.sciencedirect.com

SCIENCE DIRECT®

Solid State Ionics 176 (2005) 1291–1299

SOLID STATE IONICS

www.elsevier.com/locate/ssi

Self-assembly and flow alignment of protonically conducting complexes of polystyrene-*block*-poly(4-vinylpyridine) diblock copolymer with phosphoric acid

M. Tiitu[a], M. Torkkeli[b], R. Serimaa[b], T. Mäkelä[c], O.T. Ikkala[a,*]

[a]*Department of Engineering Physics and Mathematics, and Center for New Materials, Helsinki University of Technology, P.O. Box 2200, FIN-02015 HUT, Espoo, Finland*

[b]*Department of Physical Sciences, University of Helsinki, P.O. Box 64, FIN-00014, Helsinki, Finland*

[c]*VTT Microelectronics, Technical Research Centre of Finland, P.O. Box 1208, FIN-02044 VTT, Finland*

Received 29 September 2004; received in revised form 23 February 2005; accepted 24 February 2005

Abstract

Phosphoric acid (H_3PO_4) is selectively swollen in polystyrene-*block*-poly(4-vinylpyridine) (PS-*b*-P4VP) diblock copolymer within its P4VP domains to achieve protonically conducting self-assembled acid–base complexes. Shear flow is imposed to macroscopically align the local self-assembled structures. The materials are characterized using Fourier transformation infrared spectroscopy (FTIR), small angle X-ray scattering (SAXS), dynamic rheology, and impedance spectroscopy. Homopolymeric P4VP$(H_3PO_4)_x$ (where x denotes the nominal number of H_3PO_4 molecules vs. repeat units of P4VP) reaches the conductivity value ca. $5*10^{-3}$ S/cm at 100 °C when x approaches the values $x=2.0\cdots2.5$. By incorporating a P4VP$(H_3PO_4)_{2.2}$ block within PS-*block*-P4VP (with the block lengths 35.5 and 3.6 kD for PS and P4VP, respectively; polydispersity 1.06), lamellar protonically conducting nanochannels are formed with periodicity of ca. 450 Å based on SAXS. Large-amplitude oscillatory shear flow is applied, which leads to macroscopically rather highly aligned lamellar nanochannels based on SAXS. Surprisingly, this leads to only slightly anisotropic conductivities. For example, at 100 °C conductivity of $5*10^{-6}$ S/cm along the channels and $7*10^{-7}$ S/cm in the perpendicular direction are obtained. The observations indicate that defects, potentially involving "dead-end channels" may control the transport properties in self-assembled and aligned materials across macroscopic dimensions.

Keywords: Self-assembly; Block copolymer; Phosphoric acid; Acid–base salt; Proton conductivity; Flow alignment

1. Introduction

Proton conduction and transport has attracted considerable interest due to its scientific complexity and its importance in various technological applications and biological systems [1–5]. Water is the most studied system, and the protonic conductivity can take place by two mechanisms (see e.g. Ref. [2]). The protonated water species (such as H_30^+ and $H_5O_2^+$) can diffuse, which is denoted as the vehicular mechanism. The protons can also perform hopping in aqueous hydrogen bonded donor–acceptor chains from protonated H_3O^+ to nonprotonated H_2O, followed by their subsequent reorientation, i.e. de Grotthus mechanism [2,6]. High proton conductivity is needed e.g. for fuel cell membranes (see e.g. Ref. [4,7]). Sulfonated perfluorinated polymers [8,9] have much been used, which adsorb considerable amounts of water due to the hygroscopic nature of the grafted sulfonic acid moieties. In combination with the strong hydrophobicity of the fluorinated matrix, water-containing domains are segregated (see e.g. Ref [10]). Taken that such domains percolate, proton transport across the membrane is achieved as mediated by the adsorbed water.

There exists, however, considerable interest to develop polymeric materials whose protonic conductivity is not

* Corresponding author. Tel.: +358 50 4100454; fax: +358 9 4513155.
E-mail address: Olli.Ikkala@hut.fi (O.T. Ikkala).

0167-2738/$ - see front matter © 2005 Elsevier B.V. All rights reserved.
doi:10.1016/j.ssi.2005.02.018

based on adsorbed water [5]. In fuel cells, a desirable operating temperature is in excess of 100 °C, as hydrogen-rich feedstock, such as reformed methanol, could then be used instead of pure H_2 and the catalyst poisoning could be suppressed [11]. Therefore, alternatives for water have been searched, such as imidazole, which can similarly form hydrogen bonded chains and which can transport protons [5,12]. Proton conduction due to imidazole groups covalently connected within polymer chains has been recently demonstrated [13]. Another widely studied material is phosphoric acid [5] and its mixtures with polyethylene oxide [14], polyvinyl alcohol [15], polyacrylamide [16], and its salts with basic polymers, such as polyethyleneimine [17], poly(4-vinylimidazole) [18], and notably polybenzimidazole [19]. Closely related to the present work are poly(diallyldimethylammonium) [20] and poly(4-vinylimidazolium) [18] salts with phosphoric acid, i.e. PAMA$(H_3PO_4)_x$ and P4VI$(H_3PO_4)_x$, which behave qualitatively similarly and show relatively high conductivity as x is increased past the nominal stoichiometric value ($x=1$). For example, PAMA$(H_3PO_4)_2$, i.e. PAMA$^+(H_2PO_4)^-(H_3PO_4)$, has the conductivity of 10^{-4} S/cm at room temperature and reaches 10^{-2} S/cm at 100 °C [20]. The limiting conductivity for very large x is suggested to be that of pure H_3PO_4, which is ca. $8*10^{-2}$ S/cm at room temperature [21].

Another recent development has been to construct materials with self-assembled or even hierarchically self-assembled protonically conducting domains, leading to various functions and combinations of properties [22–25]. In the context of fuel cell membranes, self-assembly could allow means to tailor the conductivity and mechanical properties separately. Self-assembly is achieved due to competing attractive and repulsive interactions and requires well-defined structural units [26–28]. A particularly elegant system consists of undecylimidazole protonated by a small amount of monododecylphosphoric acid, which leads to lamellar self-assembly [29]. Similarly, in polymers, self-assembly and hierarchy have been obtained using block copolymers [28,30–34] and polymer complexes [25,35–37]. Typically a narrow polydispersity is required to control the structures. Sulfonated polysulfone-*block*-polyvinylidene fluoride block copolymers show interesting properties, even if only spherical phase has been reported so far [38]. Sulfonated block copolymers consisting of polystyrene and polyolefine blocks have been studied in the context of fuel cell membranes [39–42]. An example related to smart materials is polystyrene-*block*-poly(4-vinylpyridine) (PS-*b*-P4VP) where the latter block has been complexed with various sulfonic acids to render acid–base salt blocks where optionally amphiphilic alkyl phenols have been hydrogen bonded [23,24,43–45]. Hierarchical self-assembled nanostructures are obtained and the order–order and order–disorder phase transitions allow temperature driven switching of the protonic conductivity [23]. Another important aspect is that self-assembly leads only to local structures, and such polydomain structures also contain defects. In order to approach monodomain (single liquid crystalline) structures, additional fields have to be imposed, such as electric field [46,47], flow [48–50], or surfaces [51,52]. An example of the latter is PS-*b*-P4VP where the P4VP block is modified with 1,3-propane sultone, leading to cylindrically self-assembled structures, with anisotropic conductivity [53]. Notably, the film thickness has been only ca. 50 nm and the surface energies suffice to align the cylinders.

The acid–base complexes become softened when increased amounts of H_3PO_4 are added, as required for conductivity. Therefore it would be desirable to construct materials whose electrical and mechanical properties can be designed separately. Self-assembly would be a choice, taken that the alignment and connectivity of the conducting and reinforcing channels can be controlled. However, this is both a synthetic, processing, and materials design challenge when aiming at realistic materials and applications. This work concentrates on a model material of self-assembly, i.e. PS-*block*-P4VP with narrow polydispersity, where H_3PO_4 has been immobilized within the basic P4VP-block using acid–base reaction to allow PS-*block*-P4VP$(H_3PO_4)_x$. In order to align the lamellar protonically conducting domains, shear flow is used. The transport properties are studied.

2. Experimental

2.1. Materials and sample preparation

P4VP (Polysciences, $M_w=50{,}000$ g/mol), PS-*b*-P4VP (Polymer Source P98, block lengths 35,500 and 3600 g/mol, respectively; $M_w/M_n=1.06$), and H_3PO_4 (Fluka, 99%) were used. H_3PO_4 was vacuum dried (pressure 0.07 mbar) for 16 h at 25 °C before use.

Finding common solvents for PS, PS-*b*-P4VP, H_3PO_4 and their complexes to prepare blends P4VP$(H_3PO_4)_x$ and PS-*b*-P4VP$(H_3PO_4)_x$ turned out to be nontrivial. Table 1 shows the investigated solvent candidates. For solubility testing, 1.0 wt.% mixtures of P4VP/solvent and H_3PO_4/

Table 1
The observed solubilities (1 wt.%)

Solvent	P4VP	H_3PO_4	P4VP $(H_3PO_4)_x$	PS-*b*-P4VP $(H_3PO_4)_x$
Water	−	+	+	−
Ethylene glycol	+	+	+	−
Methanol	+	+	−	−
Ethanol	+	+	−	−
N,N-dimethylformamide	+	+	−	−
Benzyl alcohol	+	+	−	−
Dimethylsulfoxide	+	+	+	+ (heating)
2-Propanol	+	+	−	−
Cyclohexanol	+	+	−	−
2-Butoxyethanol	+	+	−	−
2-Ethoxyethanol	+	+	−	−

Clear solution are marked with +, phase separated mixtures with −.

solvent were prepared, mixed for 3 days, and the clarity was visually examined. If a given solvent led to separate clear solutions with P4VP and H_3PO_4, they were combined and clarity was again visually examined after a few hours. In most cases, precipitation took place at this point and the solvent candidate was abandoned. Only two solvents, i.e. dimethyl sulfoxide (DMSO) and ethylene glycol, were found to dissolve both P4VP and H_3PO_4 as well as the complex P4VP$(H_3PO_4)_x$, which was needed to prepare complexes without phase separation. Since DMSO also dissolved the used block copolymer PS-*b*-P4VP and its complexes, it was used for all the sample preparations. However, slight heating was needed in the latter case. In conclusion, use of a single solvent DMSO allowed to compare the corresponding homopolymer and block copolymer complexes.

Homopolymer complexes P4VP$(H_3PO_4)_x$ (see Scheme 1a) were prepared by dissolving P4VP and H_3PO_4 separately in DMSO (Aldrich, 99.9%) until clear (2 wt.% solutions), combining the solutions at desired fractions, and then evaporating the clear solutions on a hotplate at 100 °C. The samples were vacuum dried at 25 °C for 24 h. P4VP$(H_3PO_4)_x$ with molar fractions $x=1.0$–3.5 were prepared. More accurately, e.g. P4VP$(H_3PO_4)_3$ denotes P4VP$H^+(H_2PO_4)^-(H_3PO_4)_2$. Block copolymer complexes PS-*b*-P4VP$(H_3PO_4)_x$ with molar fractions $x=1.0$ and 2.2 (see Scheme 1b) were prepared by dissolving PS-*b*-P4VP and H_3PO_4 in DMSO at 100 °C using an oil bath. The solutions were clear, evaporated at 100 °C and vacuum dried at 25 °C for at least 24 h. All prepared complexes were homogeneous in the resolution of optical microscope.

2.2. Conductivity measurements

The conductivities were measured from cut pieces (typical size $1\times2\times0.6$ mm) in three directions with Hewlett Packard 4192LF Impedance Analyzer at frequencies 10 Hz–1 MHz using a home-made conductivity cell and parallel plate (blocking) geometry. The sample was confined between two parallel platinum plates (sizes 10×20 mm). Between the plates, there was a teflon spacer of thickness 0.5 mm with a specimen-shaped hole in it. The plates containing the teflon spacer and the sample were embedded in thermally insulating teflon around them, also containing a heater and a thermocouple. The Pt plates were electrically connected to an impedance analyzer. The sample was loaded in the following manner: the specimen was placed in the hole of the teflon spacer and the plates were tightened using screws. The system was first heated to achieve good contact between plates and the specimen, and the data collection was started thereafter. Linkam TMS 91 heating stage was employed for the temperature cycle: room temperature—155–30–155–30–155 °C. The first heating from room temperature to 155 °C took place at a rate of 5 °C/min and thereafter 1 °C/min was used in the subsequent cycling. After the first heating, the temperature was stopped for 15 min at 155 °C and subsequently at each inversion temperature for a period of 5 min. Temperature near the sample was measured using a K-type thermocouple with Fluke 80TK thermocouple module attached to a Keithley 195A Digital Multimeter. Cole–Cole plots were compiled but will not be reported here. As conventional, the conductivity was extracted from the plateau part of the conductance vs. frequency curves, see the inset of Fig. 2. Conductivity of the aligned sample was measured twice in the tangential, radial and normal directions. Each measurement was made using a fresh piece of the sample. For comparison, also the conductivities of P4VP$(H_3PO_4)_x$, $x=1.0$–3.5 were measured.

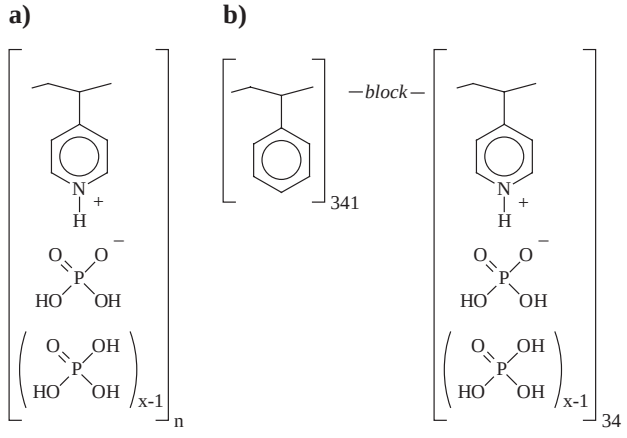

Scheme 1. P4VP$(H_3PO_4)_x$ and PS-*b*-P4VP$(H_3PO_4)_x$. The latter polymer has a narrow molecular weight distribution due to living anionic polymerization.

2.3. Rheology

Rheological measurements and large-amplitude oscillatory shear flow were performed using Bohlin CS50 stress controlled dynamic rheometer and cone and plate geometry with a 10 mm cone diameter and the cone angle 4°. Ca. 55 mg of sample was first processed with a PTFE mold and a steel press on a hotplate at 150–170 °C to form a tablet. After placing the tablet on the rheometer plate, the rheometer sample chamber was heated and kept at 150 °C for 5 min, after which the cone was brought to contact with the sample (0.150 mm gap between the tip of the cone and the plate). The amplitude and frequency sweeps were performed at different temperatures. Frequency sweeps were made in the linear regime. For large-amplitude oscillatory shear flow, a fresh sample was prepared and placed in the rheometer as described earlier. The sample was kept still at 135 °C for 1 h to achieve sufficient contact. Parameters used in the case of the sample depicted later were frequency $f=0.4$ Hz, temperature 140 °C, strain $\gamma=0.4$ and initial stress 8000 Pa. During a typical shear flow oscillation experiment, the moduli G' and G'' decreased and the phase angle δ increased. A shear flow oscillation took ca. half an hour,

after which the sample was quenched with liquid nitrogen to facilitate the detachment of the sample from the rheometer.

2.4. Small angle X-ray scattering

Small angle X-ray (SAXS) measurements were performed using a sealed fine-focus X-ray tube in the point-focus mode. CuK_α radiation ($\lambda = 1.54$ Å) was monochromatized with a Ni filter and a totally reflecting mirror (Huber small angle chamber 701) and the scattered intensity was measured with a Bruker AXS Hi-Star area detector. The distance between the sample and the detector was 117 cm. The magnitude of the scattering vector is defined as $\boldsymbol{q} = (4\pi/\lambda)\sin\theta$, where 2θ is the scattering angle. The scattering vector was calibrated using a silver behenate standard. The intensities were corrected for absorption and non-sample scattering.

2.5. FTIR spectroscopy

The Fourier transform infrared measurements were performed at room temperature with Nicolet Magna 750 FTIR spectrometer averaging 64 scans with the resolution of 2 cm^{-1}. H_3PO_4, P4VP, PS-*b*-P4VP and the polymer complexes were ground and mixed with potassium bromide (KBr Spectranal, Riedel de Haën). Pure P4VP and PS-*b*-P4VP were dissolved in DMSO, evaporated and dried the same way as the corresponding complexes before mixing with potassium bromide. The pellets were formed by pressing and vacuum dried at 25 °C for 16 h in 10^{-2} mbar vacuum before FTIR measurements.

3. Results and discussion

First, protonation of P4VP due to H_3PO_4 was demonstrated using FTIR (see Scheme 1). Fig. 1 depicts the FTIR absorption spectra at the most informative bands 1500–1700 cm^{-1} for P4VP, PS-*b*-P4VP, H_3PO_4, $P4VP(H_3PO_4)_{2.0}$ and PS-*b*-$P4VP(H_3PO_4)_{2.2}$, i.e. where the latter two complexes were selected as they have feasible conductivity properties, to be described later. Pure P4VP (Fig. 1a) has a characteristic absorption peak at 1597 cm^{-1} due to the carbon–carbon stretching of the pyridine rings. The previous results suggest that upon protonation this peak is suppressed and a shifted peak is observed at 1637 cm^{-1} [44,54]. Also the peak at 1557 cm^{-1} is suppressed due to protonation, as observed previously [54]. Therefore, Fig. 1a confirms protonation of the pyridine rings in the case of $P4VP(H_3PO_4)_{2.0}$, even if the background effect of the selected overstoichiometric amount of H_3PO_4, i.e. $x > 1$, flattens the shifted peak at 1637 cm^{-1}. In the case of PS-*b*-$P4VP(H_3PO_4)_{2.2}$ (Fig. 1b), the situation is slightly more complex, as PS-*b*-P4VP has two overlapping aromatic stretching peaks near 1600 cm^{-1} due to the pyridine rings

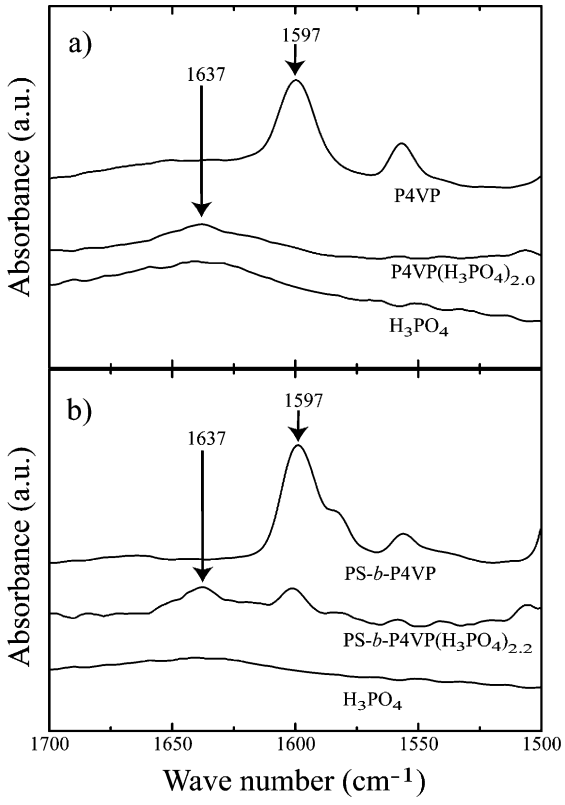

Fig. 1. FTIR absorption spectra near 1600 cm^{-1} for a) P4VP, H_3PO_4 and $P4VP(H_3PO_4)_{2.0}$ and b) PS-*b*-P4VP, H_3PO_4 and PS-*b*-$P4VP(H_3PO_4)_{2.2}$. The pyridine ring stretching at 1597 cm^{-1} and the band due to pyridinium at 1637 cm^{-1} due to proton transfer are marked with arrows.

of P4VP and the phenyl rings of PS. Upon protonation, the first one is suppressed and a shifted peak is observed at 1637 cm^{-1} whereas the absorption due to the phenyl rings of PS remains at 1600 cm^{-1}. Fig. 1b indeed shows such a behavior and confirms the protonation also in this case. FTIR does not allow to study the hydrogen bonding of the overstoichiometric H_3PO_4 to the $P4VP(H_3PO_4)_{1.0}$ salts. However, hydrogen bonding between the phosphoric acid and phosphonate moities is expected.

Fig. 2 shows the electrical conductivity of the homopolymeric complexes $P4VP(H_3PO_4)_x$ for $x = 1.0 \cdots 3.5$ vs. inverse temperature. As an example, the inset shows the conductance G for $x = 2.5$ at 36 °C as a function of frequency, and shows how the plateau value near 10 kHz allows to estimate the conductivity. At low frequencies, the electrode polarization effects dominate the behavior. Fig. 2 shows that relatively high conductivities in excess of 10^{-2} S/cm are obtained for $T > 100$ °C using higher values of x. Not surprisingly, the values are comparable with those observed for $PAMA(H_3PO_4)_x$ and $P4VI(H_3PO_4)_x$. [18,20]. To illustrate the composition dependence in more detail, Fig. 3 shows the conductivity of $P4VP(H_3PO_4)_x$ at 100 °C vs. x. The conductivity first increases relatively steeply as a function of x until $x = 2.0 \cdots 2.5$ is reached, corresponding to conductivity of ca. $5 * 10^{-3}$ S/cm at 100 °C. Beyond that x value it seems that saturation of conductivity is achieved but

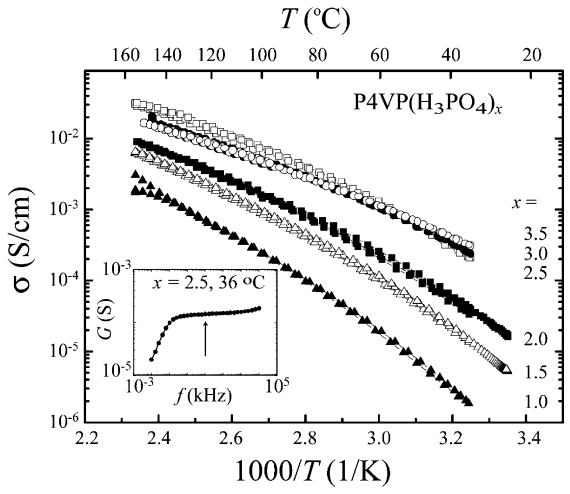

Fig. 2. Electrical conductivities of homopolymer complexes $P4VP(H_3PO_4)_x$ vs. inverse temperature. As an example, the inset shows conductance G vs. frequency f for $P4VP(H_3PO_4)_{2.5}$ at 36 °C, and the arrow indicates the plateau conductance value near 10 kHz used for evaluating the conductivity.

it is obvious that ultimately the conductivity increases slowly towards the value $8*10^{-2}$ S/cm of pure H_3PO_4 as x becomes infinite. Simultaneously, upon increasing the amount of H_3PO_4, the originally hard and brittle material becomes softened, i.e. plasticized. Fig. 2 shows that there is only a slight curvature observed in log σ vs. log $(1/T)$. In addition, at low temperatures the effect of added x is higher, i.e. adding x from 1 to 3.5 increases conductivity roughly 2 orders of magnitude at 40 °C, whereas the corresponding increase at 150 °C is only one order of magnitude. To illustrate this phenomenon, the activation energies for conductivity were evaluated from Fig. 2 using Arrhenius equation, $\sigma T = A \exp(-E_a/kT)$ where E_a=the activation energy and k=Boltzmann constant (see Fig. 4). The activation energies were relatively low, in the range 0.7 eV for $x=1$ and decreased to ca. 0.4 eV for $x=3.5$. For comparison, activation energies for phosphoric acid–doped

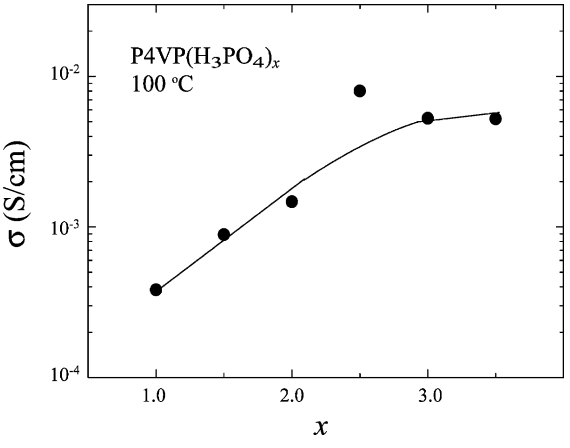

Fig. 3. Conductivity of the homopolymeric complexes $P4VP(H_3PO_4)_x$ at 100 °C vs. molar fraction of phosphoric acid, x.

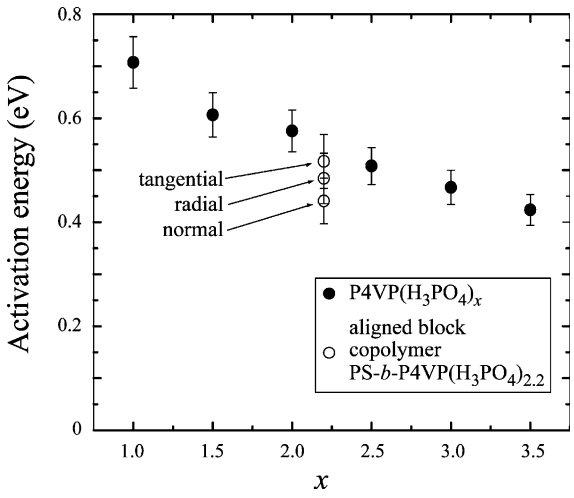

Fig. 4. Arrhenius activation energies E_a for the homopolymer complexes $P4VP(H_3PO_4)_x$ and the aligned block copolymer complex PS-*b*-$P4VP(H_3PO_4)_{2.2}$ (see later) vs. molar fraction of phosphoric acid, x.

polybenzimidazole samples vary between 0.74 [55] and 1.08 eV [56].

Fig. 3 suggests to study more closely the smallest x values that lead to "the saturation conductivity". In the complexes with the block copolymer PS-*b*-P4VP, phosphoric acid is situated in the P4VP-rich microphase. Since this microphase containing P4VP and phosphoric acid allows conductivity, it is thought that PS does not affect mechanisms inside the P4VP-rich domains and thus does not affect the needed x value for the "conductivity saturation". Therefore a proper amount of H_3PO_4 for block copolymer complexes PS-*b*-$P4VP(H_3PO_4)_x$ was chosen to be $x=2.2$ (Fig. 3) but $x=1.0$ and 0 were inspected for

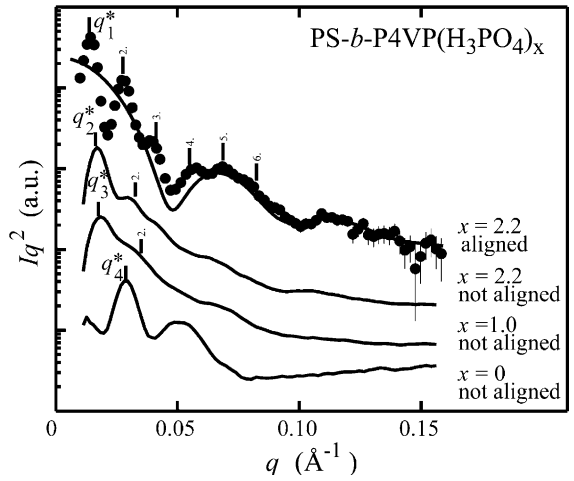

Fig. 5. Lorentz-corrected SAXS intensities vs. magnitude of scattering vector $\boldsymbol{q}$ for PS-*b*-$P4VP(H_3PO_4)_{2.2}$, PS-*b*-$P4VP(H_3PO_4)_{1.0}$ and PS-*b*-P4VP. The three lowermost curves represent samples which have not been aligned and may have considerable polydomain structure and are isotropic in the microscopic scale. The uppermost curve (shown as dots, with error bars) represents the shear aligned PS-*b*-$P4VP(H_3PO_4)_{2.2}$ where the X-ray beam is in the tangential direction, i.e. parallel to flow. The uppermost solid curve depicts the calculated structure factor for 135 Å thick lamellae with ca. 10% variations in the thickness.

reference. SAXS was used to characterize the self-assembled structures (see Fig. 5). Without any aligning procedures PS-*b*-P4VP(H_3PO_4)$_{2.2}$ showed an intensity maximum at $\boldsymbol{q}_2^*=0.016$ Å^{-1} and a second order reflection at 2 $\boldsymbol{q}_2^*$. This is indicative of a lamellar order, albeit the structure is relatively poor, probably due to a large number of defects and polydomain structure. Such behavior can be expected, as self-assembly leads only to local order. Shear flow, to be described later in more detail, was imposed to reduce defects and to render better overall order. The uppermost curve (shown as dots and the error bars indicated) represents the corresponding shear aligned PS-*b*-P4VP(H_3PO_4)$_{2.2}$ when the incoming X-ray beam was parallel to the shear flow, i.e. tangential (for the definition of the directions, see later discussion in the connection of Fig. 8). The isotropic contribution was evaluated using the radial component (see later Fig. 8) and was subtracted as a baseline where the tangential and the radial components were evaluated using radial averages within 70° sectors. Fig. 5 shows that the SAXS-reflections of the aligned PS-*b*-P4VP(H_3PO_4)$_{2.2}$ become pronounced and show intensity maxima at magnitudes of scattering vector $\boldsymbol{q}_1^*=0.014$ Å^{-1}, $2\boldsymbol{q}_1^*$, $3\boldsymbol{q}_1^*$, $4\boldsymbol{q}_1^*$, and $5\boldsymbol{q}_1^*$, confirming the lamellar self-assembly with periodicity $L_p=2\pi/\boldsymbol{q}_1^*=449$ Å. As no evidence of macroscopic phase separation was observed, it is expected that the structure consists of alternating PS and P4VP(H_3PO4)$_{2.2}$ layers. An estimate on the thickness of the polar layer can be obtained based on the structure factors. The solid curve on the aligned PS-*b*-P4VP(H_3PO_4)$_{2.2}$ data shows the calculated structure factor for 135 Å thick lamellae with ca. 10% variations in the thickness. Therefore, the PS layers would have the thicknesses of ca. 314 Å, correspondingly. Note that even if the weight fraction of the P4VP(H_3PO4)$_{2.2}$ domains is nominally only 23%, lamellar structure is obtained although the classic diblock copolymer phase diagram suggests cylindrical structure [30,31]. There is, however, probably residual DMSO solvent in the polar lamellae even after drying due to its high boiling point which effectively increases the volume fraction of the polar blocks. The intensity maxima are observed to shift to higher values of magnitude of scattering vector $\boldsymbol{q}$, i.e. smaller long periods, upon decreasing the amount of H_3PO_4: $\boldsymbol{q}_2^*=0.016$ Å^{-1} for $x=2.2$; $\boldsymbol{q}_3^*=0.018$ Å^{-1} for $x=1.0$; and $\boldsymbol{q}_4^*=0.029$ Å^{-1} for $x=0$. This is still another evidence that the added H_3PO_4 is not macroscopically phase separated but causes swelling and even structural changes of the self-assembled structures.

In conclusion, SAXS indicates that the structure of PS-*b*-P4VP(H_3PO_4)$_{2.2}$ consists of self-assembled alternating protonically conducting P4VP(H_3PO_4)$_{2.2}$ layers and insulating PS layers, see Fig. 6. As already shortly mentioned, self-assembly leads only to local order with expected residual defects and domain boundaries, in analogy with polycrystalline vs. single-crystalline order. Additional imposed fields are required to align the locally self-assembled structures [46–52] and in the present model study we use shear flow [24,45,50,57,58]. In order to understand the flow properties of PS-*b*-P4VP(H_3PO_4)$_{2.2}$, dynamic rheological properties are first characterized using oscillatory shear flow at different temperatures by applying a dynamic rheometer. As conventional, linear viscoelastic master curves are

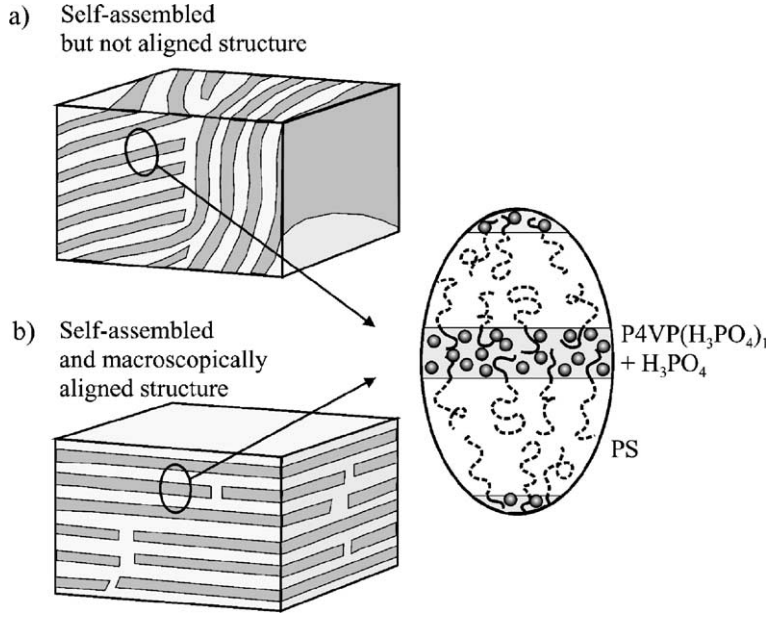

Fig. 6. Schematic picture of the self-assembled lamellar structure of PS-*b*-P4VP(H_3PO_4)$_{2.2}$. a) Self-assembly leads to local anisotropic structures but can have isotropic overall structure. b) Additional fields (such as flow) can be applied to align the local self-assembled structures to have common alignment. The structure may still have defects that cause e.g. "dead-ends" of the protonically conducting channels.

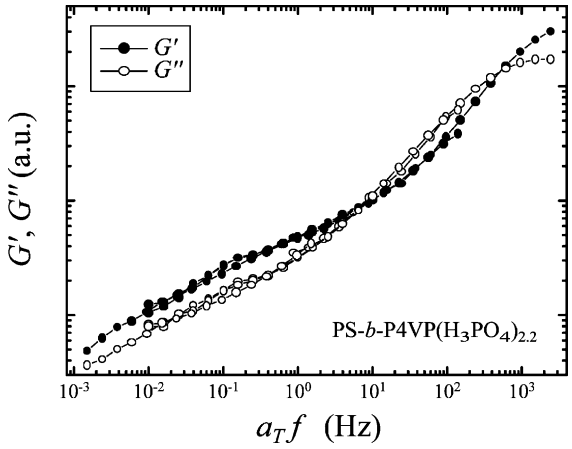

Fig. 7. Linear viscoelasticity master curves, i.e. G' and G'' vs. $a_T f$, for PS-b-P4VP$(H_3PO_4)_{2.2}$ compiled from data at temperatures 115, 125 °C, T_0=135 and 145 °C.

compiled from linear viscoelastic rheological data. In this work temperatures T=115, 125, 135 °C (=T_0), and 145 °C are used [59]. The constants C_1 and C_2 in the Williams–Landers–Ferry (WLF) equation

$$\ln a_T = \frac{C_1(T - T_0)}{C_2 + (T - T_0)},$$

can be fitted to the shift factor a_T data, and values $C_1 = -21 \pm 6$ and $C_2 = 100 \pm 20$ are obtained. Fig. 7 shows the constructed viscoelastic master curve.

Next, having understood the rheological behavior of PS-b-P4VP$(H_3PO_4)_{2.2}$, the locally ordered microphase separated domains were macroscopically aligned using large-amplitude oscillatory shear flow. The sample was sheared for about half an hour at 140 °C using frequency of 0.4 Hz and a large strain value of 0.4. During the process, the moduli G' and G'' decreased and the phase angle δ increased, as expected for shear alignment [24,45,48–50,57,58]. Two-dimensional SAXS patterns were recorded in three different directions of the incoming X-ray beam vs.

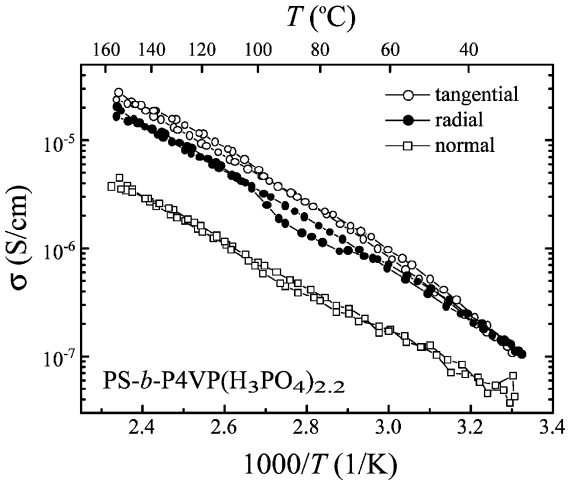

Fig. 9. Conductivities of PS-b-P4VP$(H_3PO_4)_{2.2}$ measured for the shear flow aligned sample in the tangential (along the lamellar self-assembly), the radial (along the lamellar self-assembly) and the normal (perpendicular to the lamellar self-assembly) directions vs. inverse temperature. Temperature is shown in the top axis.

the structures and show that after the shear flow, the nanostructures are macroscopically aligned (see Fig. 8). The schematics of the aligned structures are shown in Fig. 6b.

Upon shear alignment, the macroscopic structural anisotropy is expected to lead also to protonic conductivity anisotropy. The conductivities of the aligned samples were measured in the tangential, radial and normal directions vs. the shear aligned samples (Fig. 9). The conductivity is observed to be higher in the tangential and radial directions (along the lamellar protonically conducting nanochannels) than in the normal direction (across the insulating PS-layers between the lamellar protonically conducting nanochannels) but the anisotropy is only one order of magnitude and the conductivity values are low in comparison to those expected from the homopolymer complexes based on Fig. 2. The activation energies for the aligned complex are shown in Fig. 4. They seem to be of same order of magnitude or

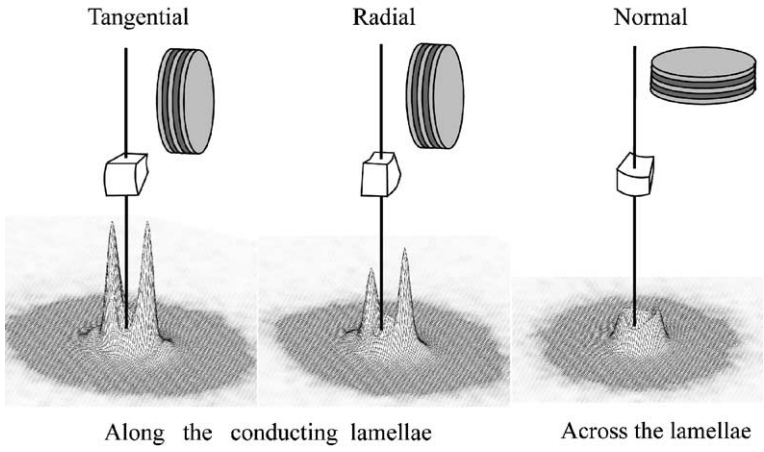

Fig. 8. Two-dimensional SAXS patterns (intensity vs. two-dimensional scattering vector) for the shear flow aligned PS-b-P4VP$(H_3PO_4)_{2.2}$ in the tangential direction (along the lamellar self-assembly), in the radial direction (along the lamellar self-assembly) and the normal direction (perpendicular to the lamellar self-assembly). The scales are linear and the peaks are observed at magnitudes of scattering vectors corresponding to those of Fig. 5.

slightly smaller than those of the corresponding homopolymer complexes. Taken the error bars, the values in the three directions are essentially similar, even if a naïve picture would suggest higher activation energies across the insulating self-assembled PS-barriers (the normal direction) in comparison to directions along the protonically conducting channels. A possible reason, albeit perhaps not the only one, is that even if two-dimensional SAXS indicates overall (macroscopic) order, there still exist domain boundaries and defects due to the insulating PS after the alignment. Thus the nanochannels are not continuous and there may be an electrical transport "leakage" between the conducting layers (see Fig. 6b). If this is the case, the results indicate the difficulty to construct continuous conducting channels over macrocopic distances, i.e. over thick membranes (see also Ref. [45]).

It is known that in sulfonated polymers, notably in the perfluorinated polymers, water-rich protonically conducting nanochannels are formed and it is important to control their percolation across the membrane. The hypothesis in the present work has been that self-assembly and alignment could allow a tractable method to design well-defined protonically conducting nanochannels. However, even if rather "open" lamellar nanochannels were used, their connectivity and continuity seems to be a complicated issue and may require ingenious techniques beyond plain self-assembly if truly percolating nanochannels with no essential dead-ends is aimed. This is particularly important taken that "thick" membranes need to be constructed, where the thickness is in the range of micrometers to millimeters. In thin films, in the range of nanometers, the surface and interface energies can be benefited, as shown before [53].

4. Conclusions

Protonically conducting self-assembled lamellar nanostructures were constructed by mixing phosphoric acid with diblock copolymer PS-*b*-P4VP having a narrow molecular weight distribution. Indirect data based on optical microscopy, FTIR, and SAXS suggests selective swelling of H_3PO_4 in the P4VP-domains, also causing protonation of P4VP. SAXS indicates lamellar order of PS-*b*-P4VP$(H_3PO_4)_{2.2}$ and shear flow was used to macroscopically align the self-assembled nanodomains, as shown by SAXS. Slight conductivity anisotropy at 100 °C was observed: $7*10^{-6}$ S/cm along the aligned nanochannels and $7*10^{-7}$ S/cm in the perpendicular direction. The conductivity level and anisotropy were much smaller than anticipated, taken the relatively high conductivity of homopolymeric P4VP$(H_3PO_4)_{2.2}$, exceeding 10^{-3} S/cm at 100 °C. This may imply the importance of the residual defects and "dead-ends" of the self-assembled protonically conducting nanochannels still existing after the flow alignment.

However, self-assembly may be important in the protonically conducting membranes as it in principle allows to control several materials properties separately, such as the conductivity and mechanical properties. In this case materials with high glass temperature above ca. 200 °C should be used for the reinforcing block. Self-assembly combined with control of the overall structure, self-assembled bicontinuous gyroid nanostructures, or "more open" molecular composite concepts where the mechanical properties are tuned by rod-like polymers [22] may offer tools to pursue to design materials from the molecular level. For fuel cell membranes, further attention has to be paid to control synthesis of block copolymers tolerant under the oxidative conditions and to increase the conductivity of their complexes with phosphoric acid.

Acknowledgements

We thank Teemu Murtola for the solubility tests, Teemu Ruotsalainen for discussions and permission to use his impedance cell, and Dr. Robin Ras for discussions. This work was carried out in the Centre of Excellence of Finnish Academy ("Bio- and Nanopolymer Research Group", 211493). Graduate schools for Materials Physics and Technical Physics of Academy of Finland are acknowledged.

References

[1] P. Colomban (Ed.), Proton Conductors, Cambridge University Press, Cambridge, 1992.
[2] K.D. Kreuer, Chem. Mater. 8 (1996) 610.
[3] M. Rikukawa, K. Sanui, Prog. Polym. Sci. 25 (10) (2000) 1463.
[4] J.A. Kerres, J. Membr. Sci. 185 (2001) 3.
[5] M.F.H. Schuster, W.H. Meyer, Annu. Rev. Mater. Res. 33 (2003) 233.
[6] N. Agmon, Chem. Phys. Lett. 244 (1995) 456.
[7] Q. Li, R. He, J.O. Jensen, N.J. Bjerrum, Chem. Mater. 15 (2003) 4896.
[8] W.G. Grot, Macromol. Symp. 82 (1994) 161.
[9] A. Steck, Membrane Materials vin Fuel Cells, in: O. Savadogo, P.R. Roberge, T.N. Veziroglu (Eds.), Proceedings of the 1st International Symposium on New Materials for Fuel Cell Systems, 1995, pp. 74.
[10] K.D. Kreuer, J. Membr. Sci. 185 (2001) 29.
[11] R. Ianniello, V.M. Schmidt, U. Stimming, J. Stumper, A. Wallau, Electrochim. Acta 39 (1994) 1863.
[12] K.D. Kreuer, A. Fuchs, M. Ise, M. Spaeth, J. Maier, Electrochim. Acta 43 (1998) 1281.
[13] H.G. Herz, K.D. Kreuer, J. Maier, G. Scharfenberger, M.F.H. Schuster, W.H. Meyer, Electrochim. Acta 48 (2003) 2165.
[14] P. Donoso, W. Gorecki, C. Berthier, F. Defendini, C. Poinsignon, M.B. Armand, Solid State Ionics 28–30 (1988) 969.
[15] S. Petty-Weeks, J.J. Zupanic, J.R. Swedo, Solid State Ionics 31 (1988) 117.
[16] J.R. Stevens, W. Wieczorek, D. Raducha, K.R. Jeffrey, Solid State Ionics 97 (1997) 347.
[17] M.F. Daniel, B. Desbat, F. Cruege, O. Trinquet, J.C. Lassegues, Solid State Ionics 28–30 (1988) 637.
[18] A. Bozkurt, W.H. Meyer, Solid State Ionics 138 (2001) 259.
[19] J.S. Wainright, J.-T. Wang, D. Weng, R.F. Savinell, M. Litt, J. Electrochem. Soc. 142 (1995) L121.
[20] A. Bozkurt, M. Ise, K.D. Kreuer, W.H. Meyer, G. Wegner, Solid State Ionics 125 (1999) 225.

[21] D.-T. Chin, H.H. Chang, J. Appl. Electrochem. 19 (1989) 95.
[22] U. Lauter, W.H. Meyer, G. Wegner, Macromolecules 30 (1997) 2092.
[23] J. Ruokolainen, R. Mäkinen, M. Torkkeli, T. Mäkelä, R. Serimaa, G. ten Brinke, O. Ikkala, Science 280 (1998) 557.
[24] R. Mäki-Ontto, K. de Moel, E. Polushkin, G. Alberda van Ekenstein, G. ten Brinke, O. Ikkala, Adv. Mater. 14 (2002) 357.
[25] O. Ikkala, G. ten Brinke, Science 295 (2002) 2407.
[26] G.M. Whitesides, J.P. Mathias, C.T. Seto, Science 254 (1991) 1312.
[27] G.M. Whitesides, B. Grzybowski, Science 295 (2002) 2418.
[28] M. Muthukumar, C.K. Ober, E.L. Thomas, Science 277 (1997) 1225.
[29] M. Yamada, I. Honma, J. Phys. Chem., B 108 (2004) 5522.
[30] F.S. Bates, G.H. Fredrickson, Annu. Rev. Phys. Chem. 41 (1990) 525.
[31] I.W. Hamley, The Physics of Block Copolymers, Oxford University Press, Oxford, 1998.
[32] S.I. Stupp, V. LeBonheur, K. Walker, L.S. Li, K.E. Huggins, M. Keser, A. Amstutz, Science 276 (1997) 384.
[33] F.S. Bates, G.H. Fredrickson, Phys. Today 52 (1999) 32.
[34] V. Abetz, Assemblies in Complex Block Copolymer Systems, in: A. Ciferri (Ed.), Supramolecular Polymers, Marcel Dekker, Inc., New York, NY, 2000.
[35] M. Antonietti, Nat. Mater. 2 (2003) 9.
[36] I.W. Hamley, Angew. Chem., Int. Ed. 42 (2003) 1692.
[37] O. Ikkala, G. ten Brinke, Chem. Comm. (2004) 2131.
[38] Y. Yang, Z. Shi, S. Holdcroft, Macromolecules 37 (2004) 1678.
[39] A. Mokrini, J.L. Acosta, Polymer 42 (1) (2001) 9.
[40] J.M. Serpico, S.G. Ehrenberg, J.J. Fontanella, X. Jiao, D. Perahia, K.A. McGrady, E.H. Sanders, G.E. Kellogg, G.E. Wnek, Macromolecules 35 (2002) 5916.
[41] J. Won, S.W. Choi, Y.S. Kang, H.Y. Ha, I.-H. Oh, H.S. Kim, K.T. Kim, W.H. Jo, J. Membr. Sci. 214 (2003) 245.
[42] J. Kim, B. Kim, B. Jung, Y.S. Kang, H.Y. Ha, I.-H. Oh, K.J. Ihn, Macromol. Rapid Commun. 23 (2002) 753.
[43] H. Kosonen, S. Valkama, J. Hartikainen, H. Eerikäinen, M. Torkkeli, K. Jokela, R. Serimaa, F. Sundholm, G. ten Brinke, O. Ikkala, Macromolecules 35 (2002) 10149.
[44] H. Kosonen, S. Valkama, J. Ruokolainen, M. Torkkeli, R. Serimaa, G. ten Brinke, O. Ikkala, Eur. Phys. J. E10 (2003) 69.
[45] T. Ruotsalainen, M. Torkkeli, R. Serimaa, T. Mäkelä, R. Mäki-Ontto, J. Ruokolainen, G. ten Brinke, O. Ikkala, Macromolecules 36 (2003) 9437.
[46] T. Thurn-Albrecht, J. Schotter, G.A. Kästle, N. Emley, T. Shibauchi, L. Krusin-Elbaum, K. Guarini, C.T. Black, M.T. Tuominen, T.P. Russell, Science 290 (2000) 2126.
[47] A. Böker, A. Knoll, H. Elbs, V. Abetz, A.H.E. Müller, G. Krausch, Macromolecules 35 (2002) 1319.
[48] Z.-R. Chen, J.A. Kornfield, S.D. Smith, J.T. Grothaus, M.M. Satkowski, Science 277 (1997) 1248.
[49] J. Sänger, W. Gronski, H. Leist, U. Wiesner, Macromolecules 30 (1997) 7621.
[50] R. Mäkinen, J. Ruokolainen, O. Ikkala, K. de Moel, G. ten Brinke, W. De Odorico, M. Stamm, Macromolecules 33 (2000) 3441.
[51] R.A. Segalman, H. Yokoyama, E.J. Kramer, Adv. Mater. 13 (2001) 1152.
[52] A. Knoll, A. Horvat, K.S. Lyakhova, G. Krausch, G.J.A. Sevink, A.V. Zvelindovsky, R. Magerle, Phys. Rev. Lett. 89 (2002) 035501.
[53] G. Cho, K.-P. Park, J. Jang, S. Jung, J. Moon, T. Kim, Electrochem. Commun. 4 (2002) 336.
[54] O. Ikkala, J. Ruokolainen, G. ten Brinke, M. Torkkeli, R. Serimaa, Macromolecules 28 (1995) 7088.
[55] H. Pu, W.H. Meyer, G. Wegner, J. Polym. Sci. Polym. Phys. 40 (2002) 663.
[56] R. Bouchet, S. Miller, M. Duclot, J.L. Souquet, Solid State Ionics 145 (2001) 69.
[57] K. de Moel, R. Mäki-Ontto, M. Stamm, O. Ikkala, G. ten Brinke, Macromolecules 34 (2001) 2892.
[58] G. Alberda van Ekenstein, E. Polushkin, H. Nijland, O. Ikkala, G. ten Brinke, Macromolecules 36 (2003) 3684.
[59] J.D. Ferry, Viscoelastic Properties of Polymers, John Wiley & Sons, Inc., New York, 1980.